J|A|C|S ARTICLES

Published on Web 01/07/2010

Mechanism of Gold Nanoparticle Formation in the Classical Citrate Synthesis Method Derived from Coupled In Situ XANES and SAXS Evaluation

Jörg Polte,[‡] T. Torsten Ahner,[†] Friedmar Delissen,[‡] Sergey Sokolov,[†] Franziska Emmerling,[‡] Andreas F. Thünemann,[‡] and Ralph Kraehnert[†,*]

Leibniz-Institut für Katalyse e.V. an der Universität Rostock, Albert-Einstein-Str. 29a, D-18059 Rostock, Germany, BAM Federal Institute of Materials Research and Testing, Richard-Willstätter-Straβe 11, D-12489 Berlin, Germany

Received August 10, 2009; E-mail: ralph.kraehnert@tu-berlin.de

Abstract: Although gold nanoparticles (GNP) are among the most intensely studied nanoscale materials, the actual mechanisms of GNP formation often remain unclear due to limited accessibility to in situ-derived time-resolved information about precursor conversion and particle size distribution. Overcoming such limitations, a method is presented that analyzes the formation of nanoparticles via in situ SAXS and XANES using synchrotron radiation. The method is applied to study the classical GNP synthesis route via the reduction of tetrachloroauric acid by trisodium citrate at different temperatures and reactant concentrations. A mechanism of nanoparticle formation is proposed comprising different steps of particle growth via both coalescence of nuclei and further monomer attachment. The coalescence behavior of small nuclei was identified as one essential factor in obtaining a narrow size distribution of formed particles.

Introduction

Gold nanoparticles (GNP) feature a wide range of potential applications in fields such as medicine,[1] biotechnology,[2] and catalysis,[3] and are thus among the most intensely studied nanoscale materials. Gold nanoparticles can be prepared via various synthesis routes including chemical, sonochemical, or photochemical paths.[4] The most common chemical route is precipitation of the GNP in aqueous solution from a dissolved gold precursor, for example $HAuCl_4$, by a reducing agent such as sodium citrate, ascorbic acid, sodium boron hydride, or block-copolymers. Whereas in most cases a further stabilizing agent is required to prevent agglomeration or further growth of the particles, some reducing agents (e.g., sodium citrate, block copolymers) also act as stabilizers. Because of its simple preparation procedure, the classical citrate method (reduction of a gold precursor with $Na_3C_6H_5O_7$ in aqueous solution near the boiling point)[5] remains one of the most reliable pathways of monodisperse gold colloids synthesis and is therefore used as a model reaction in the present study on GNP formation mechanisms.

In general, establishing control over the size and shape of nanoparticles requires a detailed understanding of the mechanism and kinetics of precursor reduction and particle growth. Although being the subject of numerous recent investigations,[6−10] a coherent mechanistic explanation for the evolution of gold particles prepared via citrate methods has not been delivered yet: Kimling et al.[6] proposed a multistep mechanism of particle formation where first the complete amount of Au(III) is quickly reduced to Au(0) atoms that form clusters, followed by their assembly into larger polycrystalline particles and completed by further aggregation. In contrast, a TEM and UV−vis-based study by Pong et al.[7] suggested that the initial fast reduction of $AuCl_4^-$ is followed by formation of clusters up to a mean radius of 2.5 nm that assemble into chains and networks of ca. 4 nm crystalline particles interconnected by amorphous gold. Those chains increase in diameter to finally collapse and cleave while at the same time individual particles grow and reach a final size of about 7.5 nm radius. Ji et al.[8] proposed a pH-dependent mechanism of particle formation, proceeding either in two steps via rapid nucleation and slow diffusion-controlled growth (pH > 6.5) or in three steps, starting from rapid nucleation, via random attachment, and finally intraparticle ripening (pH < 6.5).

Nucleation and growth processes often occur on a relatively short time scale, presenting a challenge to direct time-resolved measurements. Hence, only a few reliable accounts of the mechanism and kinetics of nanoparticles' nucleation and growth

* To whom correspondence should be addressed.
† Leibniz-Institut für Katalyse e.V. an der Universität Rostock.
‡ BAM Federal Institute of Materials Research and Testing.

(1) Copland, J. A.; Eghtedari, M.; Popov, V. L.; Kotov, N.; Mamedova, M.; Motamedi, M.; Oraevsky, A. A. *Molecular Imaging & Biology* **2004**, *6*, 341.
(2) Storhoff, J. J.; Elghanian, R.; Mucic, R. C.; Mirkin, C. A.; Letsinger, R. L. *J. Am. Chem. Soc.* **1998**, *120*, 1959.
(3) Bond, G. C.; Louis, C.; Thompson, D. T. *Catalysis by Gold*; Imperial College Press: London; 2006; Vol. 6.
(4) Daniel, M. C.; Astruc, D. *Chem. Rev.* **2004**, *104*, 293.
(5) Enustun, B. V.; Turkevich, J. *J. Am. Chem. Soc.* **1963**, *85*, 3317.
(6) Kimling, J.; Maier, M.; Okenve, B.; Kotaidis, V.; Ballot, H.; Plech, A. *J. Phys. Chem. B* **2006**, *110*, 15700.
(7) Pong, B. K.; Elim, H. I.; Chong, J. X.; Ji, W.; Trout, B. L.; Lee, J. Y. *J. Phys. Chem. C* **2007**, *111*, 6281.
(8) Ji, X. H.; Song, X. N.; Li, J.; Bai, Y. B.; Yang, W. S.; Peng, X. G. *J. Am. Chem. Soc.* **2007**, *129*, 13939.
(9) Patungwasa, W.; Hodak, J. H. *Mater. Chem. Phys.* **2008**, *108*, 45.
(10) Abecassis, B.; Testard, F.; Spalla, O.; Barboux, P. *Nano Lett.* **2007**, *7*, 1723.

 10.1021/ja906506j

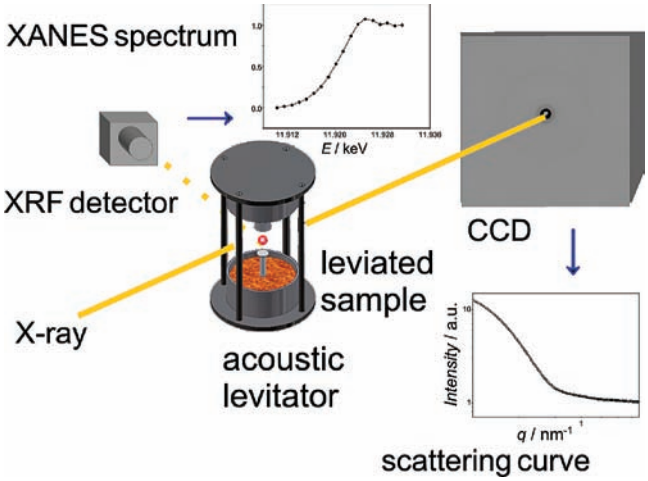

Figure 1. Schematic of the experimental setup employed for SAXS and XANES analysis on droplets of the reaction solution during GNP formation.

have been reported so far (ref 11 and references therein). Here, we used a method that analyzes levitated sample droplets with small-angle X-ray scattering (SAXS) and X-ray absorption near-edge spectroscopy (XANES) employing synchrotron radiation to directly monitor precursor reduction and nanoparticle formation. The developed setup is shown in Figure 1. The method is able to determine in situ the oxidation state of dissolved and particulate gold (XANES) concurrently with the shape, size, polydispersity, and number of the formed particles (SAXS) by probing the original colloid without further sample manipulation. Applying this analytical method-coupling in conjunction with the conventional techniques of in situ UV−vis, SEM, and TEM, the present article explores the evolution of gold nanoparticles during the classical citrate synthesis carried out at 75 and 85 °C and with different concentrations of the gold precursor.[5] On the basis of the derived comprehensive data, a mechanistic scheme for the formation of particles is proposed.

Experimental Section

Nanoparticle Synthesis. In a standard experiment, gold nanoparticles were synthesized according to the procedure described by Turkevich et al.,[5] that is chemical reduction of the gold precursor $HAuCl_4$ by dissolved trisodium citrate at 75 °C from aqueous solutions containing 0.25 and 2.5 mmol/L of gold precursor and citrate, respectively. Prior to each experiment, 35 mL aqueous (Millipore) solution of gold precursor (7 mg $HAuCl_4 \times 3H_2O$, Aldrich) and 35 mL aqueous solution of trisodium citrate (51.45 mg $Na_3C_6H_5O_7 \times 2\ H_2O$, Aldrich) were prepared and preheated to the reaction temperature. The synthesis was carried out under stirring in a flask immersed in a temperature-controlled water bath, adding the citrate solution to the gold solution. Liquid samples were extracted by pipet for SAXS/XANES, UV analysis, or pH measurement (5.8 to 6.2). For SEM imaging, ca. 0.1 mL of the final colloid was dried on a Si wafer. Additional experiments were conducted at increased temperature (85 °C) and increased initial concentration of $HAuCl_4$ (0.375 mmol/L).

Nanoparticle Characterization. At different reaction times, ca. 4 μL of the liquid samples were extracted from the batch of reaction solution and placed as droplets in an acoustic levitator (Tec5, Oberursel, Germany) applied as sample holder for X-ray analysis. The acoustic levitator was positioned in the μSpot beamline at BESSY II synchrotron (Berlin, Germany) as described in[12] to measure time-resolved combined SAXS and XANES data.[13] The employed SAXS/XANES setup is schematically depicted in Figure 1. A more detailed description of the setup and the data treatment is provided in the supplement. Significant effects of X-ray-induced reduction of the gold precursor as reported by Plech et al. were not observed.[14] (Plech et al. exposed "X-ray capillaries" filled with similar reaction solutions to synchrotron radiation and observed within 80 s the formation of particles with 12 nm radius.) Scanning electron microscopy (SEM) imaging of desiccated nanoparticles was performed on a JEOL JSM-7401F instrument operated with an acceleration voltage of 4 kV at a working distance of 2.8 mm covering the Si wafer that carried the nanoparticles with a gold mesh to reduce surface charging. Particle size and size distribution were determined from SEM images using *ImageJ* software (http://rsbweb.nih.gov/ij/) by measuring the diameter of ca. 400 particles. A Zeiss LIBRA 200-FE instrument operating at 200 kV was used for transmission electron microscopy analyses. UV−vis spectra were recorded on an Avantes AvaSpec-2048TEC-2 (Deuterium halogen light source) connected to a 10 mm optical path length cuvette holder via fiber optical cables.

Results and Discussion

A SEM image of the nanoparticles obtained upon completion of the synthesis at 75 °C is shown in part a of Figure 2. The particles' shape, size, and size distribution are in a good agreement with values reported in the literature for analogous syntheses:[6−8] particles were close to spherical and almost uniformly sized (12% polydispersity) with a mean radius of 7.6 nm (part a of Figure 2). HRTEM images of the final colloid (part c and the insert of Figure 2) reveal the crystalline nature of the particles.

UV−vis spectra recorded during the synthesis (insert in part b of Figure 2) show the evolution of an absorbance maximum in the 520 to 550 nm range, which is typically ascribed to the plasmon resonance of gold nanoparticles. During the experiment, the apparent peak maximum shifted slightly from ca. 540 nm to about 523 nm in the final colloid. The peak position is supposed to be indicative of the particle size.[6,15] The intensity at each respective maximum position of the peak is plotted in part b of Figure 2 versus time. The curve reflects the typically observed time dependency[6−8] with a slow initial intensity increase followed by a more rapid increase. Previous reports give similar accounts of the colloids measured time-resolved optical behavior and agree on the final particle size, yet the interpretation of UV data and thus the particle growth mechanism remains controversial.

Part g of Figure 2 shows the evolution of XANES spectra recorded at different reaction times; the average oxidation state calculated from XANES data is given in part h of Figure 2. The curve indicates an initially slow reduction process but a strong decrease in the Au(III) content after ca. 50 min, which coincides with the rapid increase in the intensity of the GNPs plasmon resonance observed by UV−vis (part b of Figure 2). The XANES data were analyzed by fitting each spectrum as a linear combination of the experimentally derived spectra of the initial state (precursor solution) and the final state (precursor

(11) Finney, E. E.; Finke, R. G. *J. Colloid Interface Sci.* **2008**, *317*, 351.
(12) Wolf, S. E.; Leiterer, J.; Kappl, M.; Emmerling, F.; Tremel, W. *J. Am. Chem. Soc.* **2008**, *130*, 12342–12347.
(13) Paris, O.; Li, C. H.; Siegel, S.; Weseloh, G.; Emmerling, F.; Riesemeier, H.; Erko, A.; Fratzl, P. *J. Appl. Crystallogr.* **2007**, *40*, S466.
(14) Plech, A.; Kotaidis, V.; Istomin, K.; Wulff, M. *J. Synchrotron Radiation* **2007**, *14*, 288.
(15) Haiss, B.; Thanh, N. T. K.; Aveyard, J.; Fernig, D. G. *Anal. Chem.* **2007**, *79*, 4215.

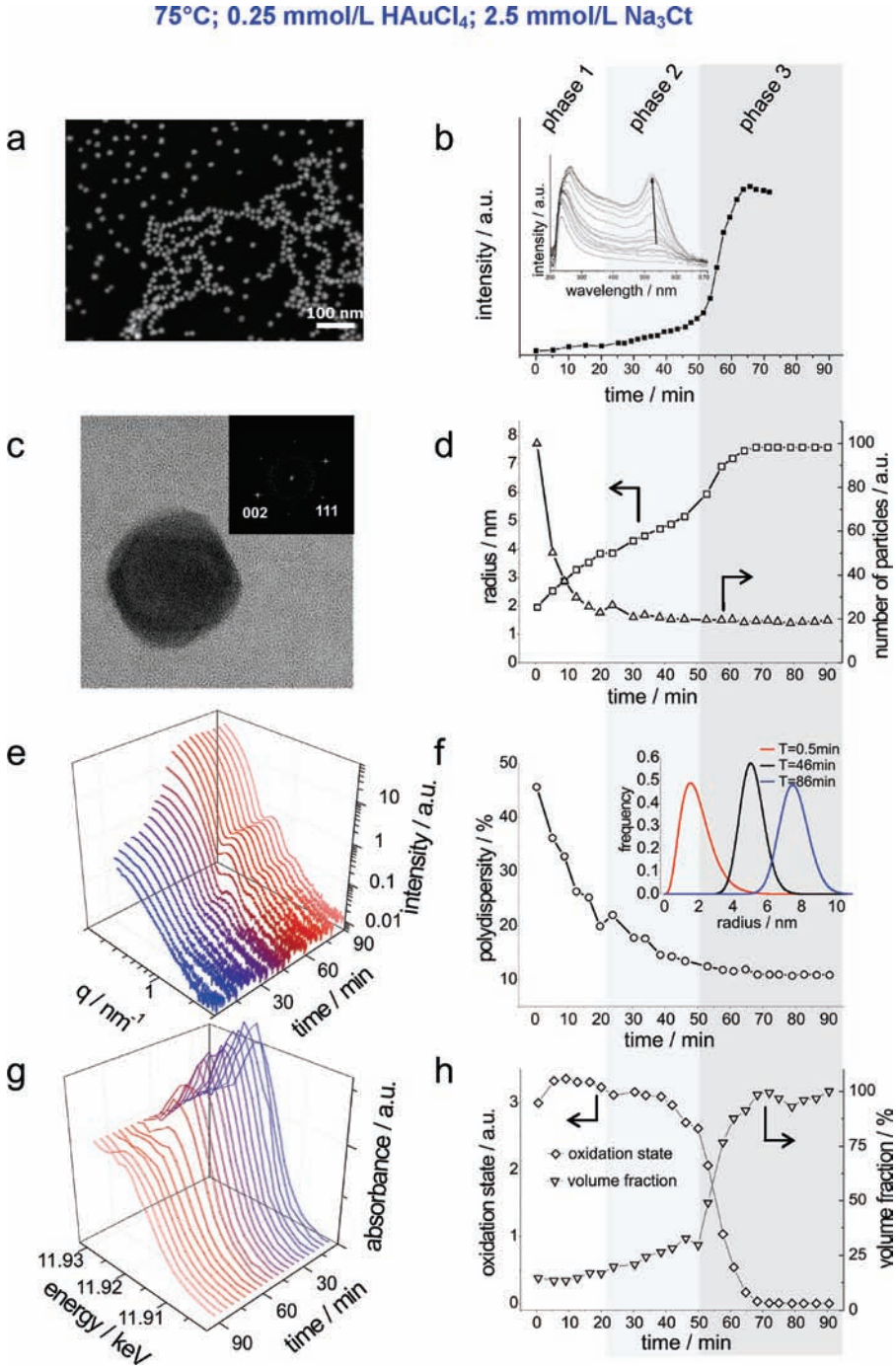

Figure 2. SEM, UV, TEM, SAXS, and XANES data on formation of gold nanoparticles (GNP) at 75 °C reaction temperature: a) SEM image of the final GNP. b) UV−vis spectra recorded during GNP formation (insert) and intensity of plasmon resonance band vs time. c) TEM image of the formed GNP. d) Mean sphere radius and normalized number of particles plotted vs reaction time derived from SAXS. e) Series of SAXS scattering curves recorded during GNP synthesis. f) Polydispersity of particles as a function of time and corresponding particle size distribution of the Schulz−Zimm distribution exemplarily shown for three reaction times (insert). g) Series of XANES spectra recorded during GNP synthesis. The diminishing of the pre-edge peak indicates the reduction of Au(III) to Au(0). h) Average formal oxidation state of gold derived from normalized XANES spectra plotted vs reaction time; volume fraction of particles calculated from SAXS data.

fully converted into particles). To those states a formal oxidation state of Au(III) and Au(0) was assigned, respectively. As a first approximation, this average oxidation state resulting from the fitting procedure can be interpreted as the fraction of gold contained in the solution, which has not been converted yet into metallic Au(0) by chemical reduction. It has to be noted that the assigned oxidation states are formal values relating to the initial and final state of reacting gold, and not necessary absolute and precise values, because uncertainties exist for the absolute oxidation state of gold in the reference spectrum for Au(III). According to Ji et al.,[8] the dissolved precursor can exist in the form of $AuCl_4^-$, $AuCl_3(OH)^-$, $AuCl_2(OH)_2^-$, $AuCl(OH)_3^-$, or $Au(OH)_4^-$, depending on pH. The corresponding exchange between Cl and OH in the coordination sphere around gold certainly affects the electron distribution in the ion, and with an increasing number of OH^- the gold will appear slightly more oxidized. The resulting small initial change in the oxidation state is also experimentally observed: when joining the reacting

solution pH of the precursor, the solution increases due to dilution with the citrate solution. Hence, a slight shift up in the oxidation state can be seen, most likely corresponding to the exchange of chloride and hydroxide from $AuCl_4^-$ to $AuCl_3(OH)^-$ (part h of Figure 2, first and second points) before the oxidation state then decreases due to the progressing chemical reduction of the gold precursor into metallic gold.

Part e of Figure 2 presents corresponding SAXS scattering curves obtained during the same experiment. The characteristic colloid properties deduced from evaluated SAXS data are given in part d of Figure 2 (particles' mean radius and number), f (polydispersity and particle size distribution (insert)), and h (volume fraction of particles). Measured scattering curves along with the corresponding fits are provided in the supplement (Figure S2 of the Supporting Information). Each experimental data point corresponds to a fresh sample extracted from the reacting batch solution, with each sample droplet being exposed for ca. 130 s to the incoming X-ray beam. The time resolution of the measured combined SAXS/XANES data amounts to ca. three minutes, that is data acquisition time plus the time required to exchange the sample droplet.

The experimental evidence derived from in situ UV, XANES, and SAXS reveals different phases of nanoparticle formation as marked on the joined time scale of parts b, d, f, and h of Figure 2. The first phase starts with a rapid nucleation process: As indicated by SAXS (particle volume fraction in part h of Figure 2), about 20% of the gold precursor is transformed into nuclei or particles within the first 60 s of the synthesis. Those particles initially show a mean radius of 2 nm and are rather polydisperse (SAXS: 45% polydispersity, part f of Figure 2). The subsequently decreasing number of particles (SAXS: part d of Figure 2) suggests that the nuclei merge and aggregate within 20 min to particles with 4 nm mean radius, while at the same time the polydispersity decreases to 20%. This increase in particle size is accompanied by a slow reduction process, evidenced by the consumption of Au(III) (XANES: part h of Figure 2), suggesting that coalescence[16] or Ostwald ripening[17] are the main mechanisms responsible for particle growth at this stage. Keeping in mind that at this point more than 90% of the particles feature radii bigger than 1 nm, dissolution of particles seems to be unlikely. Hence, the first synthesis phase constitutes a fast nucleation with a formation of nuclei ($\langle r \rangle = 2$ nm) and coalescence of these particles within 20 min to particles with 4 nm mean radius.

In a second growth phase taking place between 25 and 50 min, SAXS data indicate that particles grow continuously to a mean radius of 5.2 nm (part d of Figure 2) and the polydispersity decreases down to 14% (part f of Figure 2), whereas the number of particles remains almost constant (part f of Figure 2). This behavior is in accordance with the so-called "focusing effect" or "growth by diffusion" model first described by Reiss et al.[18,19] In this model, the growth rate of spherical particles depends solely on the monomer flux supplied to the particles and thus the polydispersity decreases during the growth. However, such a diffusion regime occurs typically on a time scale of several seconds, not minutes or even hours as in the present study. This discrepancy can be explained by the results of XANES measurements, which indicate that the corresponding reduction rate, that is the change in the concentration of Au(III) precursor, is slow (part h of Figure 2). This implies that the reduced gold is growing onto the particles by diffusional growth, but because the reduction rate is low the chemical reduction of the gold precursor becomes the limiting factor and determines in consequence the nanoparticle's growth rate.

The third phase (50−70 min) includes a rapid consumption of the remaining Au(III) species (ca. 70%, part h of Figure 2) accompanied by an increase in the particle size and a further decrease of polydispersity to 10% (part f of Figure 2), resulting in a final GNP mean radius of 7.6 nm. The accelerated consumption of Au(III) observed after 50 min and at about 5 nm GNP radius can possibly be attributed to an autocatalytic reduction on the surface of the formed nanoparticles. Interestingly, ca. 5 nm is also the size where the advent of bulk properties is discussed for GNP in literature.[4]

To proof the more general validity of the experimentally observed phases of gold nanoparticle growth and the corresponding interpretation of the data, a simple kinetic study was carried out for the synthesis process varying two of the critical parameters, that is the reaction temperature and the concentration of the gold precursor in the reaction solution. In both cases, the reduction of the gold precursor and the growth on GNP were followed with XANES and SAXS, respectively. In a first experiment, the reaction temperature was raised from 75 to 85 °C. Corresponding SAXS and XANES data are presented in parts a (particles mean radius and number), b (polydispersity) and c (volume fraction of particles, average oxidation state) of Figure 3 (also, see Figure S3 of the Supporting Information in the supplement for scattering curves and fits). The data show qualitatively the same behavior as observed at 75 °C, that is the rapid initial formation of small particles, a subsequent decrease in number of particles and polydispersity, and finally a slow and then rapid growth of particles until complete conversion of the gold precursor. In comparison with the reference experiment (Figure 2), it is obvious that each phase of the reaction proceeds significantly faster at the higher temperature, leading to completion of the reaction in about half the time as compared to 75 °C. This increase in formation rate suggests that the reduction of Au(III) proceeds faster; thus the reduction of the gold precursor is an activated chemical process.

In yet another kinetic experiment, the initial concentration of gold precursor was increased from 0.25 to 0.375 mmol/L, whereas the reaction temperature remained unchanged at 75 °C. Corresponding SAXS and XANES data are shown in parts d (particles mean radius and number), e (polydispersity) and f (volume fraction of particles; average oxidation state) of Figure 3 (see Figure S4 of the Supporting Information for scattering curves and fits). As already observed for the increased temperature, also the increased initial concentration of gold precursor significantly accelerates the process of GNP formation. Nevertheless, the phases of formation are the same as already discussed. The clear increase in particle growth rates indicates that in the chemical reaction of reducing the Au(III) precursor the reaction order for the gold precursor is significantly higher than one. Noteworthy is that in this experiment also the initial increase in particle radius (the first two points in part d of Figure 3) could be captured by the SAXS analysis because the first sample droplet was extracted slightly earlier from the reactor (0.5 min instead of 1.0 min) than in the preceding experimental runs. That this initial increase can indeed be observed experimentally suggests that also the first particle formation step, that

(16) Mandal, M.; Ghosh, S. K.; Kundu, S.; Esumi, K.; Pal, T. *Langmuir* **2002**, *18*, 7792.
(17) Madras, G.; McCoy, B. J. *J. Chem. Phys.* **2002**, *117*, 8042.
(18) Reiss, H. *J. Chem. Phys.* **1952**, *20*, 1216.
(19) Peng, X. G.; Wickham, J.; Alivisatos, A. P. *J. Am. Chem. Soc.* **1998**, *120*, 5343.

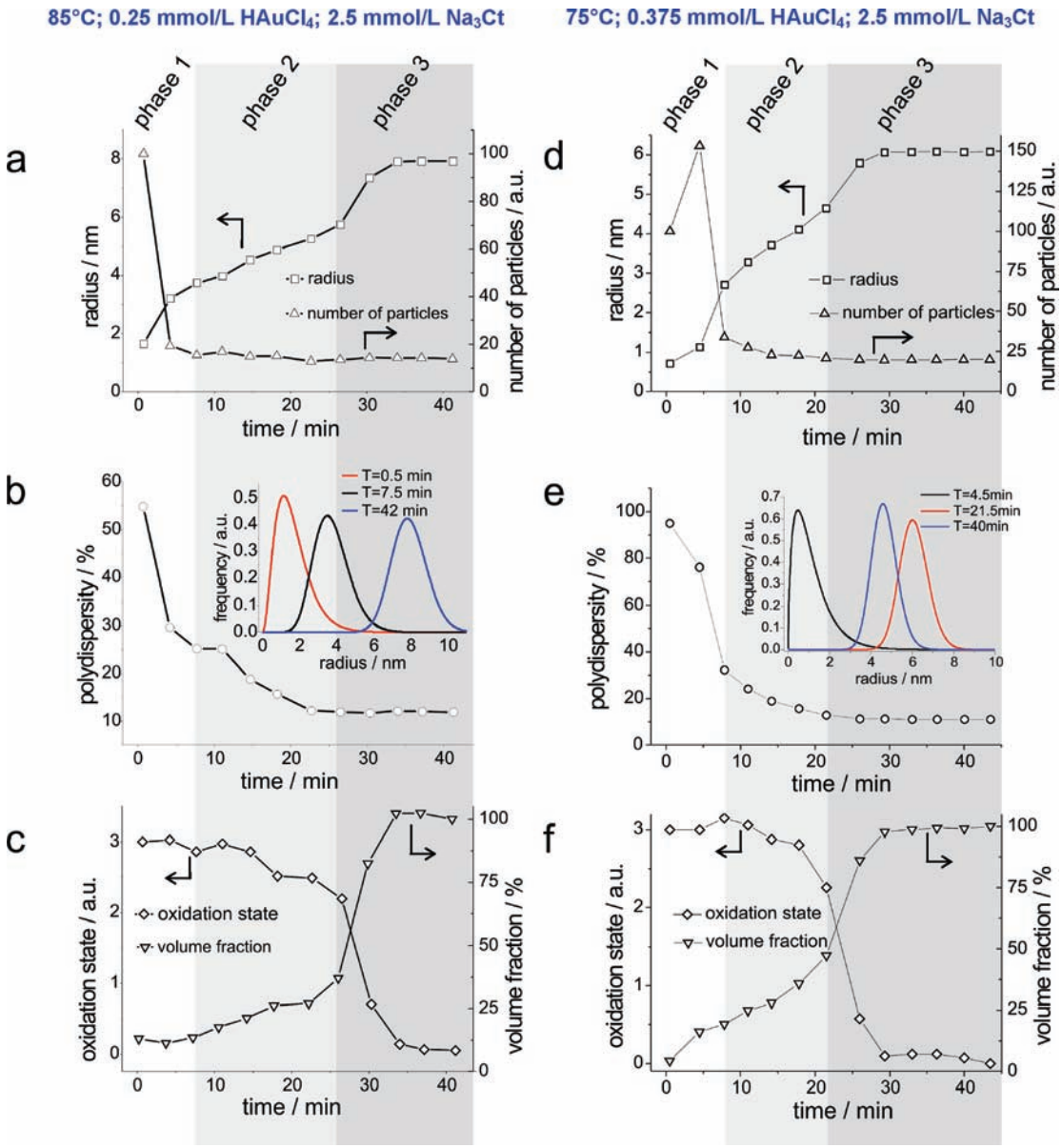

Figure 3. SAXS and XANES data on the kinetics of gold nanoparticles' formation at increased reaction temperature (85 °C: parts a, b, and c), and at 75 °C but with increased concentration of gold precursor (1.5 fold, cHAuCl4 = 0.375 mmol/L: parts d, e, and f) with otherwise unchanged synthesis parameters. a,d) Mean sphere radius and normalized number of particles plotted vs reaction time derived from SAXS. b,e) Polydispersity of particles as a function of time and corresponding particle size distribution of the Schulz−Zimm distribution exemplarily shown for three reaction times (insert). c,f) Average formal oxidation state of gold derived from normalized XANES spectra plotted vs reaction time; volume fraction of particles calculated from SAXS data.

is particle nucleation, occurs on a time scale of several seconds and not instantaneously. Thus, increasing the time resolution of the analytical methods in the initial stage of the synthesis experiment might allow us to follow the particle nucleation process in a quantitative manner.

The three phases of GNP formation observed experimentally at different reaction conditions can be interpreted as a four-step nucleation and growth process, whereas the initial phase can be divided into two steps. The initial stage is a rapid formation of nuclei (step a in Figure 4) followed by coalescence of the nuclei into bigger particles (step b in Figure 4). The third step comprises slow diffusion growth of particles sustained by ongoing reduction of gold precursor as well as a further coalescence (step c in Figure 4). Subsequently, particles grow rapidly to their final size, the final particle size being imposed by complete consumption of the precursor species (step d in Figure 4).

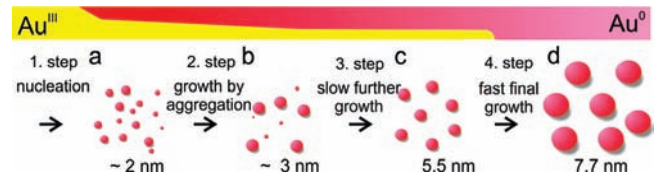

Figure 4. Schematic illustration for the deduced process of gold nanoparticle formation.

The presented experiments suggest a sequential process of GNP formation that deviates from previously proposed mechanisms.[6,7] Specifically, our novel in situ XANES and SAXS analysis confirmed neither the earlier proposed initial complete reduction of Au(III) nor the intermediate presence of networks of partially crystalline gold nanowires suggested by Pong et. al.[7] In contrast, we observed a rapid initial reduction of only a fraction of the precursor, with both coalescence as

well as further precursor reduction contributing to a different extent to the particle growth at different stages of the GNP formation process. Although one can describe the initial step as burst nucleation, the growth mechanism proposed in the present article is not in complete agreement with the classical nucleation theory by LaMer.[20] In his classical theory, the formation of primary particles is described as a self-nucleation process at the initial stage, where the formed nuclei act as seeds for the particle growth. A characteristic feature of such a process is the initial increase of particle number that then remains constant from a certain time of the reaction (when the supersaturation is too low to form new nuclei). Contrarily, the present data suggest that in the citrate synthesis of GNP the number of particles decreases significantly within 20 min after the nucleation accompanied by particle growth but only minor Au(III) consumption, suggesting a coalescence of particles. Moreover, in contrast to the current view that control over nucleation and growth are key factors in the synthesis of monodisperse GNP, we found strong indications that coalescence processes of small nuclei into monodisperse particles are essential for obtaining GNP of low polydispersity.

Conclusions

The applied combination of SAXS and XANES analysis provides time-resolved in situ information on the formation of gold nanoparticles that was previously not accessible with the conventional techniques usually applied in studies of nanoparticle formation. From the combined data, a four-step mechanism of GNP formation is proposed. Particles are formed through a sequence of reaction steps comprising fast initial formation of small nuclei, coalescence of the nuclei into bigger particles, slow growth of particles sustained by ongoing reduction of gold precursor, and subsequent fast reduction ending with the complete consumption of the precursor species. The coalescence of small nuclei into monodisperse particles plays a vital role throughout the synthesis reaction and determines the polydispersity of the formed colloid. Increasing either the reaction temperature or the initial concentration of gold precursor accelerates the particle formation process significantly. Challenges for future studies are an improved time resolution of the analytical method, a variation of synthesis conditions in a broader range to derive comprehensive kinetic information, and comparative studies on the formation mechanisms of other metal nanoparticles to elucidate if the proposed mechanism of nanoparticle formation can be generalized.

Acknowledgment. R.K. acknowledges generous funding from the BMBF within the frame of the NanoFutur program (FKZ 03X5515). We thank Simone Rolf from BAM for technical assistance and Dr. Anna Fischer from the Max Planck-Institute for Colloid Research for providing the TEM images.

Supporting Information Available: Additional details on the procedures of nanoparticle synthesis as well as recording and treatment of SAXS and XANES data, and SEM images of GNP are shown as well as measured and fitted SAXS curves for all experiments. This material is available free of charge via the Internet at http://pubs.acs.org.

JA906506J

(20) Lamer, V. K. *Ind. Eng. Chem.* **1952**, *44*, 1270.
(21) Bare, S. R.; Modica, F. S.; Ringwelski, A. Z. *J. Synchrotron Radiation* **1999**, *6*, 436.
(22) Fernandez-Garcia, M. *Catal. Rev.—Sci. Eng.* **2002**, *44*, 59.